JOURNAL OF APPLIED ELECTROCHEMISTRY **26** (1996) 129–134

Effect of magnetic charging of Ni on electrolytic codeposition of Zn with Ni particles

R. A. TACKEN, P. JISKOOT, L. J. J. JANSSEN

Department of Chemical Engineering, Laboratory of Instrumental Analysis, Eindhoven University of Technology, PO Box 513, 5600 MB Eindhoven, The Netherlands

Received 3 October 1994; revised 27 March 1995

Composite materials with unique properties can be produced by codepositing an inert phase during a cathodic metal deposition process. The feasibility of codeposition is mainly determined by the interaction of the inert phase and the cathodically deposited metal. When both the inert phase and the cathode or the cathodically deposited metal are ferromagnetic substances, codeposition can be promoted by magnetizing the inert phase prior to codeposition. Codeposition of Zn with Ni particles on a steel cathode from a weakly acidic zinc chloride based bath was investigated. The increased interaction between the magnetically remanent Ni particles and the steel cathode resulted in substantially higher percentages of Ni included in the deposit layer, especially at low concentrations of Ni particles in the bath. The model of Guglielmi, modified for conducting particles, proved to be valid; the value of adsorption parameter k_{ad} changed with magnetic remanency. Cathodic Zn deposition efficiency decreased with increasing concentration of Ni particles in solution and increasing Ni content in the deposit. The principle outlined can also be applied to systems with nonferromagnetic inert phases by coating these with ferromagnetic substances.

List of symbols

A_G	constant (Guglielmi) (V^{-1})
B_G	constant (Guglielmi) (V^{-1})
B	magnetic field flux density (T)
B_r	remanent magnetic field flux density (T)
c_p	concentration particles in bath ($kg\,m^{-3}$)
d_d	deposit layer thickness (m)
F	Faraday's constant ($C\,mol^{-1}$)
H	magnetic field strength ($A\,m^{-1}$)
i	current density ($A\,m^{-2}$)
i_0	exchange current density ($A\,m^{-2}$)
k_{ad}	Langmuir adsorption constant
M	magnetization ($A\,m^{-1}$)
M_r	remanent magnetization ($A\,m^{-1}$)
n	valence of deposited metal
V_p	volume of particles deposited per area of electrode surface (m)
W	molecular weight ($kg\,mol^{-1}$)
X_p	weight percentage of Ni in deposit
Y_p	volume percentage particles in bath

Greek symbols

α_p	volume fraction of Ni in deposit
η	overpotential (V)
η_c	cathodic efficiency
μ_0	magnetic permeability of vacuum ($V\,s\,A^{-1}\,m^{-1}$)
$\nu_{p,0}$	constant for particle deposition ($m\,s^{-1}$)
ρ_m	density of metal matrix ($kg\,m^{-3}$)
θ	degree of strong adsorption coverage
σ	degree of loose adsorption coverage

1. Introduction

Composite materials with unique properties can be produced by codepositing an inert phase during a cathodic metal deposition process. The composite obtained possesses combined properties of the two deposited materials. Several combinations have proved to exhibit enhanced wear resistance (e.g., Ni–SiC), corrosion (e.g. Ni–Si_3N_4, Zn–Al_2O_3) or lubrication properties (e.g., Ni/PTFE).

The electrolytic codeposition process is affected by a large number of process parameters [1]. The exact influence of each of these parameters is not clear; contradictory results have been reported. However, the electrostatic interaction between the inert phase and the cathodically deposited metal matrix seems to be one of the key factors determining the feasibility of the codeposition [2, 3]. An inert particle with a negative surface charge will hardly codeposit on the negatively charged cathode. To improve codeposition by means of changing the inert particle surface charge, surfactants and specific ions have been used [2, 4, 5]. The use of surfactants especially influences the structure of the composite layer adversely, because the surfactants are also included during the codeposition process. We have developed a new method that greatly improves the interaction between inert phase and cathode or cathodic layer, without using additives. The method is based on magnetically charging the inert phase.

When a magnetic field H is applied to a ferromagnetic material, the magnetic flux density B induced in the material is amplified as a result of magnetization M of the sample, and is expressed by [6]

$$B = \mu_0(H + M) \tag{1}$$

On removing the applied field H, B shows a hysteresis effect; a certain remanent magnetic flux density B_r, which is proportional to the remanent magnetization M_r, remains in the ferromagnetic material. From Equation 1 and for $H = 0$:

$$M_r = B_r/\mu_0 \tag{2}$$

Codeposition increases to a great extent using a magnetically remanent inert phase and a cathode or cathodically depositing metallic matrix of a material with high magnetic permeability. Increased affinity of the magnetized particles to the cathode is caused by two effects. First, it is energetically favourable for the particles to close their magnetic field lines going through a medium with a high magnetic permeability such as a steel cathode (or a depositing Fe or Ni matrix). Secondly, a magnetic dipole–dipole interaction between already included particles and free particles in solution is present. Because of the short range character of magnetic forces, the method outlined will not enhance transport of particles to the cathode to a large extent, but will have the effect of adsorbing the particles more strongly to the cathodic surface once arrived there.

We chose Zn deposition with Ni particles on a ferromagnetic steel cathode as a model system for this new method. Besides its experimental suitability, the main criterion for its selection, this system also has practical relevance: Zn–Ni layers with approximately 12% Ni exhibit excellent corrosion resistant properties and can serve as a corrosion protective layer on steel. However, these are difficult to electrochemically deposit at high speed as an alloy because deposition is of the anomalous type [7–9]. Codeposition of Ni particles with Zn, followed by heat treatment could be an interesting alternative route for obtaining Zn–Ni alloys.

Nickel powder was magnetized before codepositing it in a Zn-matrix on a steel cathode. The increased interaction between the magnetically remanent Ni particles and the highly magnetically permeable steel cathode resulted in substantially higher weight percentages of Ni in the deposit. This effect was most pronounced at low concentrations of Ni particles in the bath. A slightly modified form of Guglielmi's model for codeposition [10] was used to fit the experimental results.

2. Experimental details

2.1. *Reagents and experimental setup*

All plating experiments were performed in a 600 ml beaker using a three-electrode setup and electrochemical interface (Autolab PGSTAT20, Eco Chemie Utrecht). A Zn bar (10 cm^2 surface area) was used as the anode. The reference electrode was a saturated calomel electrode (SCE) connected to the cell by a Luggin capillary. A strip of steel (Bonder Prüfbleche EN10130 $FePO_4$, Chemetall GmbH Frankfurt) with an exposed area of 4 cm^2 was used as the working electrode (cathode), and was positioned vertically and opposite the anode at a distance of 7 cm. Prior to plating, the steel cathode was degreased in a solution of 15 $kg\,m^{-3}$ Alfecu SF600 (Akzo Nobel), 0.53 M NaOH, 0.084 M $Na_2CO_3 \cdot 10H_2O$, 0.059 M $Na_2HPO_4 \cdot 12H_2O$ and 0.01 M sodium dodecylsulphate at 50 °C for 10 min. Thereafter, it was rinsed with distilled water, etched for 5 min in 4 M HCl, and rinsed again with distilled water.

A zinc chloride bath was prepared by dissolving 0.22 M $ZnCl_2$ and 3.36 M NH_4Cl in millipore filtered water. The pH was adjusted to 5.8 by addition of concentrated ammonia. All experiments were carried out at room temperature. Before codeposition experiments, the zinc chloride bath was purified by potentiostatic preelectrolysis using a ribbed Ti-cathode of 9 cm^2 and applying a potential of −1.2 V vs SCE for 15 min. Commercially available Ni-powder (Merck) with a size distribution of 1 to 10 μm was used. The mean particle diameter was 4 μm, as determined on a particle size analyser (Coulter LS). Prior to codeposition, the Ni-powder was magnetized in a rectangular copper solenoid. Particle size distribution was not seen to have changed after magnetization treatment (no clustering of particles). During codeposition experiments, the solution was stirred mechanically to keep the Ni particles in suspension. The stirring rate was kept constant to ensure that the hydrodynamic conditions were identical for every experiment. Codeposition experiments were started immediately after addition of (magnetized) Ni powder to the zinc chloride bath. In every figure that will be presented, the total charge consumed at the cathode is identical for each sample; the actual layer thickness is, however, a function of both cathodic efficiency and amount of particles included.

The field strength produced by the solenoid used was measured with a Hall probe. Nickel powder magnetization curves were measured at room temperature on a vibrating sample magnetometer (Princeton model 155): starting with a sample with magnetization $M = 0$, a certain field H was first applied and then removed. After the remanent magnetic moment was determined the sample was again forced into the unmagnetized state by applying a H field with diminishing amplitude (going to zero) and alternating polarity. This procedure was repeated while H was increased.

2.2. *Analysis of Zn–Ni layers*

The Zn–Ni composite layers deposited were dissolved in concentrated HNO_3, in which the underlying steel cathode surface passivates. Using an atomic absorption spectrophotometer (Perkin–Elmer 4995), both

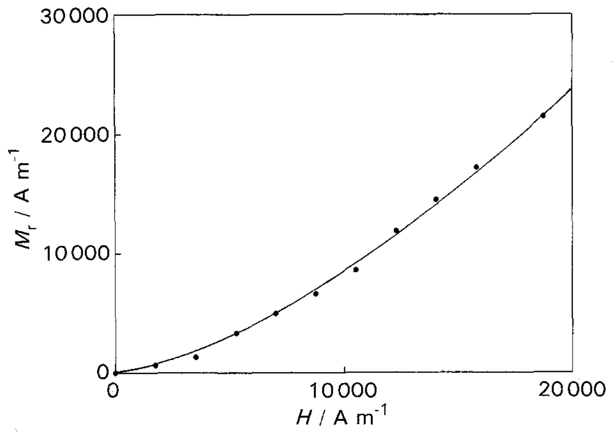

Fig. 1. Dependence of remanent (volume) magnetization of Ni powder, M_r, on the strength of the applied magnetizing field H.

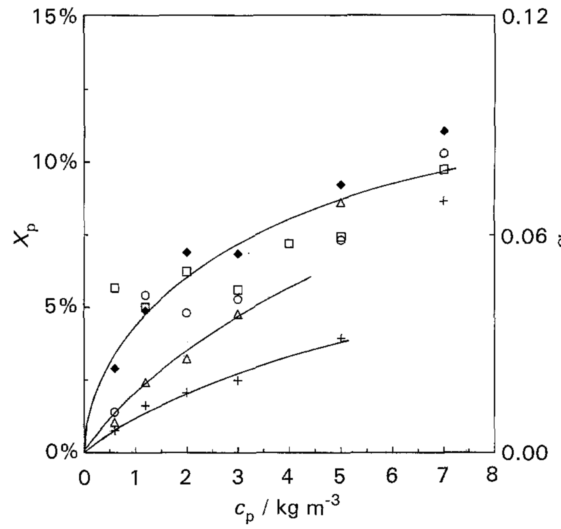

Fig. 2. Dependence of weight percentage included Ni in the Zn–Ni composite layer, X_p, on Ni particle concentration in the bath. Several data points are averaged values of two or three measurements. The Ni particles have remanent magnetizations M_r of: (+) 0, (△) 3300, (◆) 8600, (○) 17200 and (□) 34000 A m^{-1}; $i = 300$ A m^{-2}; $t = 420$ s. Lines are drawn for $M_r = 0$, $M_r = 3300$ and $M_r > 3300$ A m^{-1}.

Ni^{2+} and Zn^{2+} concentrations were analysed to calculate composition of the deposited layers and current efficiency. Both surface and cross-sectioned scanning electron microscopy photographs of the deposited Zn–Ni layers were taken. Cross sections were prepared by first cutting the samples transversely, then embedding them in a Perspex/Cu matrix, polishing and carefully etching. A Cambridge stereoscan 200 scanning electron microscope was used.

3. Results and discussion

3.1. *Ni powder remanent magnetization curve*

Nickel powder remanence as a function of H is depicted in Fig. 1. The initial nonlinearity of the curve is a result of the reversible character of the magnetization process at low fields. It appears that remanence, M_r, is of the same order of magnitude as the strength of the applied H field (during application of H magnetization M of the Ni sample is of course much higher). Although remanent magnetization is presented here as a bulk property, it is in fact dependent on the size and structure of each particle. From the fact that the magnetic moment did not decrease over a period of two hours, it was concluded that it was justified to regard the remanent magnetization as being a static property.

3.2. *Effect of Ni powder magnetization on codeposition*

After magnetization, the Ni powder was codeposited with Zn in the Zn plating bath. The Ni content of the deposited composite layer as a function of both concentration of Ni powder in the bath and remanent magnetization of the powder is depicted in Fig. 2.

Although the data points show some scatter, the effect of remanent magnetization is undoubtedly there. The shape of the curves drawn resembles Langmuir type adsorption isotherms, as predicted by the model of Guglielmi [10]. This model, one of the earliest on codeposition, has proved to be very useful for practical applications, although several parameters influencing codeposition are not taken into account. The model was originally set up for non-conducting particles, but because of the high electrical conductivity of the Ni particles used, a slightly modified version of the model is developed in this study. Guglielmi's model is based on the assumption that codeposition is a two-step adsorption process; the first step is a physical (loose) adsorption of the particles, the second a field-assisted strong adsorption. Guglielmi supposes the dependence of loose adsorption σ on the concentration (volume percentage Y_p) of particles in the bath to resemble Langmuir isotherms:

$$\sigma = \frac{k_{ad} Y_p}{1 + k_{ad} Y_p}(1 - \theta) \tag{3}$$

The term $(1 - \theta)$ describes the fraction of the surface available for establishment of the particle's strong adsorption equilibrium. Although a conducting particle, after being strongly adsorbed to the cathode, can immediately be covered by depositing metal and, therefore, is available for establishment of the equilibrium again, the term $(1 - \theta)$ is maintained in the case of conducting particles. This is because, due to hydrodynamic forces, strong adsorption of a particle on top of another strongly adsorbed particle will hardly occur unless that particle is almost fully embedded in the growing metal matrix and is not a high spot on the electrode surface any longer (this is confirmed by the absence of both dendritic growth and clustering of particles on SEM-photographs, Section 3.3).

The adsorption constant, k_{ad}, essentially depends on the intensity of particle/cathode interaction and normally has a fixed value for a specific type of inclusion particle in a specific codeposition system. In our experiments, k_{ad} changes by inducing magnetic remanency in the Ni particles. The method outlined by Guglielmi is based on the assumption that strong

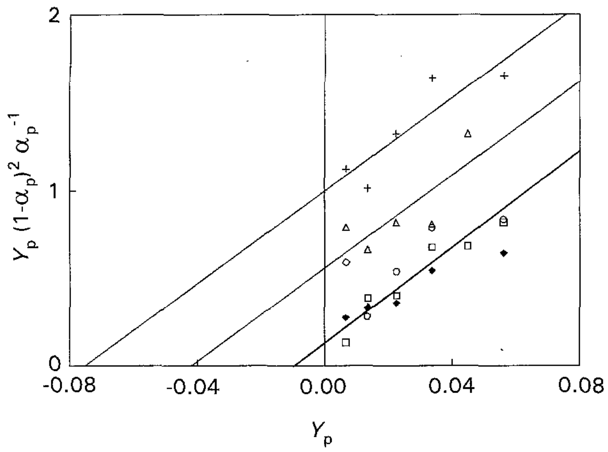

Fig. 3. Modified Guglielmi plot for determination of adsorption constant k_{ad}. All data are taken from Fig. 2, restricted to $\alpha_p < 0.08$; (+) $M_r = 0$, (△) 3300, (◆) 8600, (○) 17 200 and (□) 34 000 A m^{-1}. Lines are drawn for $M_r = 0$, $M_r = 3300$ and $M_r > 3300$ A m^{-1}.

adsorption of the particles to the cathode is an electric field dependent process. By analogy with Butler–Volmer electrode kinetics, this dependence is considered to be exponential:

$$\frac{dV_p}{dt} = \sigma \nu_{p,0}\, e^{B_G \eta} \quad (4)$$

Different from Guglielmi's model for nonconducting particles, the term $(1 - \theta)$ is dropped in Tafel's law since the whole electrode surface is available for metal deposition:

$$i = i_0\, e^{A\eta} \quad (5)$$

Combination of Equations 3, 4, 5 and Faraday's law leads to

$$\frac{\alpha_p}{1-\alpha_p} = \frac{nF\rho_m \nu_{p,0}}{Wi_0}\, e^{(B_G - A_G)\eta}\, \frac{k_{ad} Y_p (1-\theta)}{1 + k_{ad} Y_p} \quad (6)$$

Assuming spherical particles or particles of reasonably regular shape, θ has almost the same value as α_p. Rearranging Equation 6 then yields:

$$\frac{Y_p (1-\alpha_p)^2}{\alpha_p} = \frac{Wi_0}{nF\rho_m \nu_{p,0}}\, e^{(A_G - B_G)\eta} \left(\frac{1}{k_{ad}} + Y_p\right) \quad (7)$$

Under the galvanostatic conditions used in the present experiments, overpotential η remains fairly constant if the amount of strongly adsorbed conducting particles is small. For small α_p, k_{ad} can be found graphically by plotting $Y_p(1-\alpha_p)^2\alpha_p^{-1}$ against Y_p. This is depicted in Fig. 3 for the data of Fig. 2. The cutoff at the x-axis equals $-(1/k_{ad})$. Note that one line has been drawn for the data with $M_r = 8600$, 17 000 and 34 000 A m^{-1}.

The slopes of the drawn lines are expected to be equal. However, it may be possible that the parameters $\nu_{p,0}$ and B_G, which influence the slope, change with M_r. The model of Guglielmi is not straightforward with respect to the physical meaning of these parameters. In Table 1, values for k_{ad} and the loose adsorption coverage, σ, of the cathodic surface for a Ni particle concentration of 2 kg m^{-3} is calculated using Equation 3 and assuming $\theta = \alpha_p$.

Table 1. Values of k_{ad} for Ni powders with different magnetic remanency M_r and degrees of loose adsorption, σ, at $c_p = 2\,kg\,m^{-3}$. $i = 300\,A\,m^{-2}$; $t = 420\,s$

M_r/A m^{-1}	k_{ad}	σ at $c_p = 2\,kg\,m^{-3}$
0	13.3	0.23
3300	23.8	0.34
8600–34000	90	0.64

Figure 4 shows the dependence of the codeposition process on current density at different values of powder magnetization. Experiments with current densities below 100 A m^{-2} were not carried out but a maximum in the curve is likely to arise. The literature [11] reports the occurrence of such a maximum at an overpotential (and accordingly current density) where the surface charge of the cathode is minimized. This results in minimum ordering of water dipoles at the electrode which benefits codeposition.

To study the role of the steel cathode on the magnetic phenomena observed, the following experiment was conducted. On a series of steel cathodes, pure Zn layers with increasing thicknesses d_{Zn} were electrodeposited. On top of these layers, 8 μm of Zn–Ni composite layer was deposited. In this way, a fixed distance initially separated the steel surface from the solution. The pure Zn layer served as a barrier for interactive magnetic effects. The effect of this distance on weight percentage Ni in the composite layer is given in Fig. 5. Note that the inclusion percentages are mean values over the layers of 8 μm thick. The influence of the steel cathode on the inclusion process appears to extend over a distance of approximately 15 μm. The magnetic attraction force perpendicular to the electrode surface, decreasing with increasing layer thickness, increases the residence time of Ni particles at the cathode surface and, consequently, promotes inclusion. It is expected that a gradient in particle concentration develops in the deposit: a decrease in particle concentration with increasing distance to the steel surface.

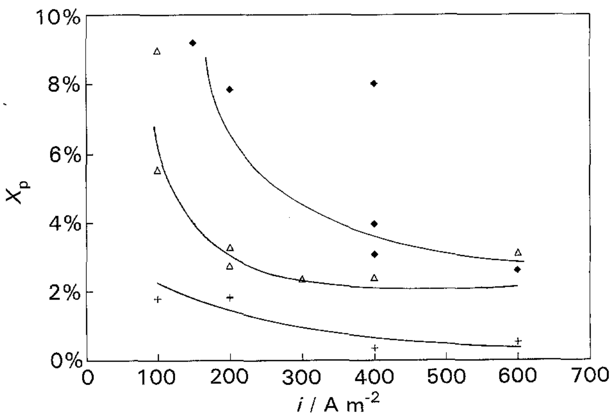

Fig. 4. Dependence of the weight percentage included Ni in the Zn–Ni composite layer on plating current density for three differently magnetized Ni powders: (+) $M_r = 0$, (△) 3300 and (◆) 8600 A m^{-1}; $c_p = 1.2$ kg m^{-3}; $it = 168\,000$ A s m^{-1} (corresponding to a layer thickness of about 8 μm).

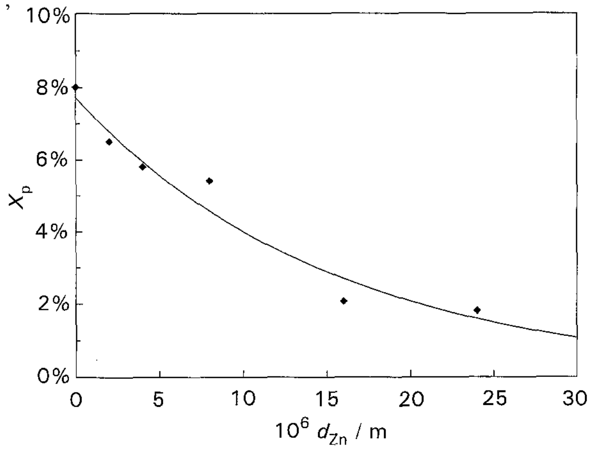

Fig. 5. The weight percentage Ni in the Zn–Ni composite layer as a function of the thickness of a pure Zn layer deposited on a steel cathode. The composite layer was deposited on top of a pure Zn layer with $i = 400\,\mathrm{A\,m^{-2}}$; $t = 420\,\mathrm{s}$; $c_p = 1.2\,\mathrm{kg\,m^{-3}}$ and $M_r = 8600\,\mathrm{A\,m^{-1}}$.

3.3. *Mechanistic information from SEM-photo analysis and current efficiency measurements*

There are a large number of processes playing a role in the inclusion of magnetized Ni particles. The fact that these are electrically conductive contributes to the complexity of the codeposition process. Only a few publications on codeposition of electrically conducting particles can be found in the literature [12, 13]. Surface and cross-section SEM-photo analysis reveal qualitative information. Figure 6 shows a typical example of the surface of a plated composite Zn–Ni layer. Since the sample was thoroughly rinsed, all particles that are still visible are immobilized and strongly adsorbed on the Zn matrix. The upper surface of some Ni particles is totally uncovered, while others are covered with a mossy Zn deposit. This mossy, open Zn structure is probably caused by competitive hydrogen gas evolution. In addition, passivation of the Ni particles may prohibit the formation of sound Zn deposits on the Ni particles. As a consequence, the mechanical bonding between particles and matrix is not expected to be very strong.

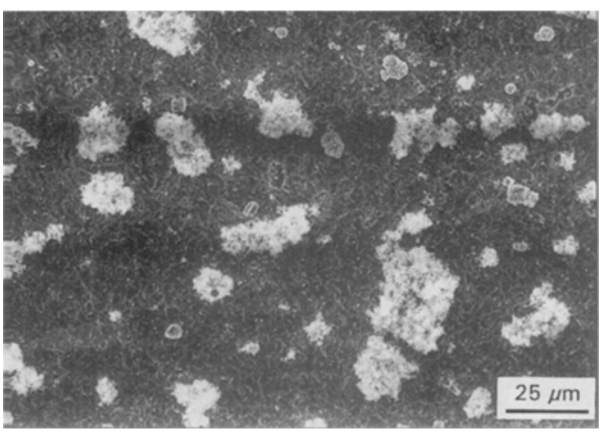

Fig. 6. Surface photograph of Zn–Ni composite layer; $i = 250\,\mathrm{A\,m^{-2}}$; $t = 1600\,\mathrm{s}$; $c_p = 0.6\,\mathrm{kg\,m^{-3}}$; $M_r = 3300\,\mathrm{A\,m^{-1}}$, magnification 660×.

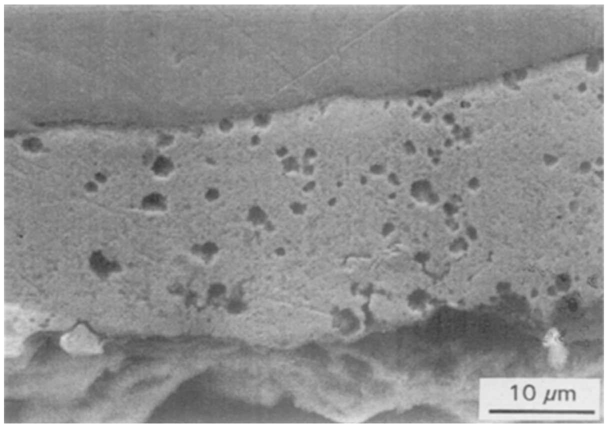

Fig. 7. Cross-section photograph of Zn–Ni composite layer, upper layer is steel; $i = 400\,\mathrm{A\,m^{-2}}$; $t = 1317\,\mathrm{s}$; $c_p = 2\,\mathrm{kg\,m^{-3}}$; $M_r = 8600\,\mathrm{A\,m^{-1}}$; magnification 2040×.

Detailed analysis of Fig. 6 and similar photographs shows a small gradient in concentration of holes over the deposit layer: higher concentrations are found closer to the steel surface. Clustering of particles seems to be absent; it appears that magnetic dipole–dipole interactions between Ni particles are not predominant, but the attraction between the remanent particles and the highly magnetically permeable steel substrate is. This is supported by the fact that the magnetic permeability of the steel is much higher than that of Ni powder [6].

The places where Ni particles were situated originally, appear as holes in the cross-section photograph of Fig. 7. Due to the weak mechanical anchoring, the particles have been torn out of the composite layer during polishing. When breaking out of the layer, it is possible that the particles take along part of the (mossy) Zn deposit around them.

Cathodic current efficiency measurements show a decrease in cathodic efficiency as a function of the concentration of Ni particles in the bath (η_c decreases from about 100% to about 85% when c_p increases to $7\,\mathrm{kg\,m^{-3}}$). A clear correlation between cathodic efficiency and magnetic remanency M_r was not found. Both c_p and M_r influence X_p, the weight percentage of Ni codeposited (η_c decreases from about 100% to about 85% when X_p increases to 10%). Several processes affect efficiency. Firstly, hydrogen will evolve very much faster on a Ni particle in the Zn–Ni deposit than on Zn due to the low exchange current density on the latter. This process is expected to be linearly related to X_p (and consequently to c_p and M_r). Secondly, cathodic efficiency, as determined by dissolution of the obtained composite layer, can be lowered by Zn deposition and hydrogen evolution on Ni particles that are temporarily strongly adsorbed (make electrical contact) at the cathode, that is, particles that are not included but again move into suspension after a certain time. Zn present on these detached Ni particles will corrode. This process influences efficiency, particularly at high c_p and M_r. Thirdly, conducting particles colliding with an electrode will be charged and, due to their capacitance, will discharge in the electrolyte when the contact between particle and electrode is broken. As a result of the dependency of the variables in question, it is difficult to clarify the process, or processes, causing reduced cathodic efficiency.

4. Final remarks

In the present work, compared to conventional codeposition methods, several extra parameters influencing the inclusion process are encountered. The magnitude of magnetic remanency of the particles, deposit thickness (determining the distance between free particles and cathode supporting material) and magnetic properties of the cathodic substrate and depositing matrix metal are additional factors to be considered.

Nickel was used successfully in this study, although it is classified as a soft magnetic material and, consequently, is expected to exhibit only negligible magnetic remanency. It is known, however, that small particles possess magnetic properties different from the bulk material [6]. This is believed to result from the high degree of shape and/or crystal anisotropy that these small particles possess, which prevents magnetic domain walls to return to their original energetically most favourable positions after the removal of an externally applied magnetic field.

The principle outlined in this paper can be applied to any system with an at least partially ferromagnetic inert phase that exhibits magnetic remanency. The inert phase can be a ferromagnetic pure element (Ni, Fe, Co), but also an alloy or other magnetic compound (e.g., Fe_3O_4 or Fe_3Si). Further, nearly every type of inert phase can be coated electrolessly with a ferromagnetic metal layer (using, for example, N_2H_4 as a reductor) to make it sensitive to magnetization so that electrolytic codeposition can be influenced beneficially.

References

[1] J. P. Celis and J. R. Roos, Proc. AES Techn. Conf. SUR/FIN '84, New York, 16–19 July, paper 0-1 (1984).
[2] J. P. Celis, PhD thesis, KU Leuven, Belgium (1976).
[3] J. Fransaer, J. P. Celis and J. R. Roos, *J. Electrochem. Soc.* **139**(2) (1992) 413.
[4] K. Helle, *Adv. Org. Coat. Sc. and Techn.* **2** (1979) 264.
[5] T. W. Tomaszewski, L. C. Tomaszewski and H. Brown, *Plating* **56** (1969) 1234.
[6] B. D. Cullity, 'Introduction to magnetic materials', Addison–Wesley, Cambridge, MA (1972).
[7] E. Chassaing and R. Wiart, *Electrochim. Acta* **37** (1992) 545.
[8] R. Fratesi and G. Roventi, *J. Appl. Electrochem.* **22** (1992) 657.
[9] L. Felloni, R. Fratesi, E. Quadrini and G. Roventi, *ibid.* **17** (1992) 574.
[10] N. Guglielmi, *J. Electrochem. Soc.* **119** (1972) 1009.
[11] J. Fransaer, J. P. Celis and J. R. Roos, *ibid.* **139** (1992) 413.
[12] R. Bazzard and P. J. Boden, *Trans. Inst. Met. Finish.* **50** (1972) 63.
[13] S. W. Watson and R. P. Walters, *J. Electrochem. Soc.* **138** (1991) 3633.